| | |
|---|---|
| Title | Numerical Investigation of Magnetic Resonant Coupling Technique in Inter-Chip Communication via Electromagnetics-TCAD Coupled Simulation |
| Author(s) | Chen, Q; Ho, SL; Fu, WN |
| Citation | IEEE Transactions on Magnetics, 2012, v. 48 n. 11, p. 4253-4256 |
| Issued Date | 2012 |
| URL | http://hdl.handle.net/10722/189053 |
| Rights | IEEE Transactions on Magnetics. Copyright © IEEE. |

# Numerical Investigation of Magnetic Resonant Coupling Technique in Inter-Chip Communication via Electromagnetics-TCAD Coupled Simulation

Quan Chen, S. L. Ho, and W. N. Fu

Department of Electrical Engineering, Hong Kong Polytechnic University, The University of Hong Kong, Pokfulam, Hong Kong

**Wireless power transfer based on magnetic resonant coupling (MRC) has attracted extensive studies for its applications in macroscopic engineering. In this work, we explore one potential application of MRC in microelectronics, i.e., as an enhancement of inductive coupling for wireless inter-chip communication. Theoretical analysis and numerical simulation are conducted to study the advantages of MRC in power transfer efficiency. In particular, a new EM-semiconductor simulator is employed to provide a faithful description for the interactions between magnetic fields and semiconductor carrier transport.**

*Index Terms*—**EM-TCAD simulation, inductive inter-chip communication, magnetic resonant coupling.**

## I. Introduction

In recent years, wireless energy transfer via magnetic resonant coupling (MRC) has been attracting increasing attention. As a short- to mid-range wireless energy transfer technique first reported in 2007 [1], [5], MRC uses *non-radiative* magnetic fields to transmit energy efficiently between two resonant objects. The transfer efficiency can reach 40% for distance up to 8 times the radius of the transmitting coil [1], which is several orders higher than traditional inductive power transfer. Extensive studies have been carried out to investigate the applications of MRC in remote charging of mobile devices and biomedical implantable devices [2], [3].

While being widely used in macroscopic applications, the MRC technique has also great potentials in microelectronic areas. One typical application is using MRC as an enhancement for inductive inter-chip communication for three-dimensional (3D) integration circuits (ICs), where signal is transferred wirelessly among different silicon layers via inductive coupling, as shown in Fig. 1. Although on-chip inductive communication is regarded a promising substitute for existing interconnect structure and under active development, the power efficiency of traditional inductive coupling drops with $1/d^3$ as distance $d$ increases, which limits the effective communication distance to be less than the inductor diameter to avoid excessive power consumption [4].

In addition, in 3D stacks of chips, the magnetic fields will be further weakened by eddy current when penetrating through semiconductor substrate. Therefore, to maintain a sufficient signal strength at the receivers several "substrates" away from the transmitters, larger inductors or transceiver arrays (large coil diameter), thinner chip substrate (smaller distance) and/or higher input power are required. This imposes challenges to the applicability of the technique given the tight area and power budgets for on-chip designs.

Manuscript received March 02, 2012; accepted April 08, 2012. Date of current version October 19, 2012. Corresponding author: Q. Chen (e-mail: alexandercq@gmail.com).

Color versions of one or more of the figures in this paper are available online at http://ieeexplore.ieee.org.

Digital Object Identifier 10.1109/TMAG.2012.2195300

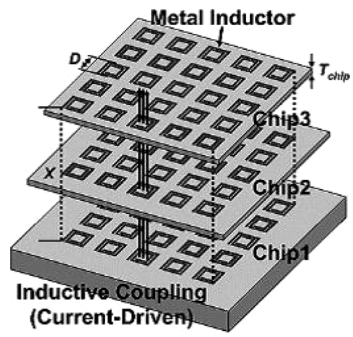


Fig. 1. Inductive inter-chip communication [4].

When modeling inter-chip wireless communication, the response of semiconductor to magnetic fields, which is more complicated than that of metal and insulator, requires special attention. Standard EM solvers such as HFSS typically simplify semiconductors as conductors with equivalent conductivity. This equivalent conductivity, however, is difficult to be determined accurately. A number of influential factors specific to semiconductors, e.g., field dependent mobility, charge generation/recombination and electron/hole hall effects and doping density/homogeneity, cannot be described in such treatment of semiconductors. Standard semiconductor device simulators, on the other hand, usually neglect the magnetic effects. Since typical on-chip communication frequency is in GHz, the interactions between EM fields and semiconductor carrier transport become prominent, which calls for a simultaneous account of the two dynamics in one single simulation framework.

In this paper, we explore the feasibility of using the MRC technique to enhance the power efficiency of inter-chip wireless communication, thereby reducing chip area and energy consumption. Numerical simulations are conducted to study the performance characteristics of MRC inter-chip transfer and demonstrate its advantages. In particular, a 3D simulator Magwel [9], which solves concurrently the full-wave Maxwell's equations and the technology computer-aided design (TCAD) semiconductor model, is employed to extract coupling coefficients among different inductors with semiconductor substrates located in between the transmission path. To the best of the

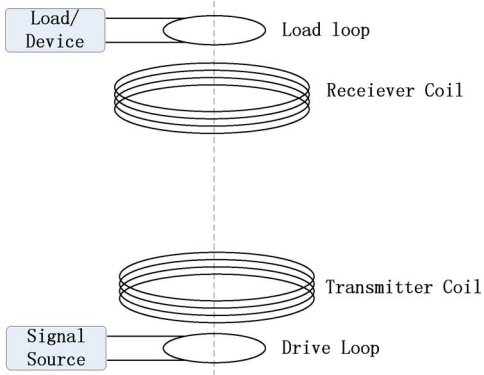


Fig. 2. MRC-based wireless inter-chip communication structure.

authors' knowledge, this is the first reported study of applying MRC technique in the context of microelectronic applications.

## II. On-Chip Signal Transfer via MRC

The proposed MRC system for on-chip signal transfer is depicted in Fig. 2. Differing from the traditional inductive coupling, the MRC system has a drive loop at the bottom layer and a load loop on the top layer, which constitutes the transmitter and the receiver with the TX coil and the RX coil in the middle, respectively. The source generator is connected to the drive loop, from which power is transferred to the TX coil via normal (non-resonant) inductive coupling. The receiver side functions in a similar manner. The load is connected to the load loop, which extracts energy from the RX coil inductively. The TX and RX coils are both RLC resonant circuits, between which energy can be transferred in high efficiency when they resonate at the same frequency. By isolating the drive (load) loops and the TX (RX) coils, the source (load) resistance can be transformed into a much higher effective resistance in parallel with the RLC resonant tank of the TX (RX) coil, there providing a higher quality (Q) factor for energy transfer [2]. Note that adding the drive and load loops represents only a minor increase in implementation complexity and is easy to realize with current fabrication technology.

The equivalent circuit of the proposed system is shown in Fig. 3. The coil resistances $(R1 - R4)$ are calculated by the common conductor resistance formula. The high-frequency effect on resistance is neglected since the small cross-section diameter is comparable to the skin depth at GHz range. The four self-inductances $(L_1 - L_4)$ are determined analytically by the modified Wheeler formula [6]. Since the distance between any pair of coils is generally no greater than the coil diameter, all six magnetic coupling coefficients $(k_{12}, k_{23}, k_{34}, k_{13}, k_{24}, k_{14})$ have to be taken into account. The separation between the TX (RX) coil and the drive (load) loop is fixed, so is $k_{12}$ $(k_{34})$. The other four cross-coupling coefficients are functions of the communication distance, the intermediate materials and the coil geometry. The two adjustable capacitors $C_2$ and $C_3$ are used to tune the resonant frequency.

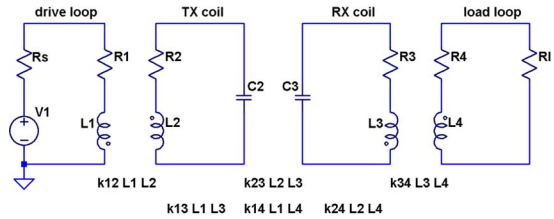


Fig. 3. Equivalent circuit model.

By writing the Kirchhoff's voltage law for each loop, the following equations can be obtained [2]

$$\begin{aligned} V_S &= (R_S + R_1)i_1 + j\omega\Lambda_1 \\ 0 &= \left(R_2 + \frac{1}{j\omega C_2}\right) i_2 + j\omega\Lambda_2 \\ 0 &= \left(R_3 + \frac{1}{j\omega C_3}\right) i_3 + j\omega\Lambda_3 \\ 0 &= (R_4 + R_L)i_4 + j\omega\Lambda_4 \end{aligned} \tag{1}$$

where $\Lambda_1$ through $\Lambda_4$ represent the magnetic flux linkages in each of the four coils. The flux linkages are related to the current variables by a $4 \times 4$ symmetric inductance matrix

$$\begin{bmatrix} \Lambda_1 \\ \Lambda_2 \\ \Lambda_3 \\ \Lambda_4 \end{bmatrix} = \begin{bmatrix} L_{11} & M_{12} & M_{13} & M_{14} \\ M_{12} & L_{22} & M_{23} & M_{24} \\ M_{13} & M_{23} & L_{33} & M_{34} \\ M_{14} & M_{24} & M_{34} & L_{44} \end{bmatrix} \begin{bmatrix} i_1 \\ i_2 \\ i_3 \\ i_4 \end{bmatrix} \tag{2}$$

where $M_{xy}$ denotes the mutual inductance between $L_x$ and $L_y$. The coupling coefficients are defined by $k_{xy} = M_{xy}/\sqrt{L_x L_y}$, and extracted from the imaginary part of Z-parameters obtained by stand-alone simulation of the corresponding pair of coupled inductors. Once the circuit parameters (R, L and C) and the six coupling coefficients are known, (1) and (2) can be solved simultaneously to obtain the current variables and the load voltage $V_L = i_4 R_L$ as well. The $\|S_{21}\|$ parameter can be computed by

$$\|S_{21}\| = 2\frac{V_L}{V_S}\sqrt{\frac{R_S}{R_L}}. \tag{3}$$

## III. EM Simulation Without Semiconductor

First, a high-frequency EM simulator Ansoft HFSS, is employed to analyze the characteristics of the proposed four-coil structure, in the absence of semiconducting medium. The TX and RX coils are multi-turn square spiral while the drive and load loops are single-turn square loops. The geometric specifications of the four coils are given in Table I. The calculated inductance of TX coil is 4.2 nH. The two lumped capacitors are set to be 1 pF, making the resonant frequency to be 2.45 GHz. For simplicity, the system is defined to be symmetric, i.e., $k_{12} = k_{34}$ and $k_{13} = k_{24}$. The four independent coupling coefficients are extracted from the HFSS simulation. For different communication distances, $k_{12} = 0.63$ is fixed. The dependence of the other three coefficients on the communication distance $d$ is shown in Fig. 4. Fig. 5 shows the simulated $|S_{21}|$ curve of the four-coil

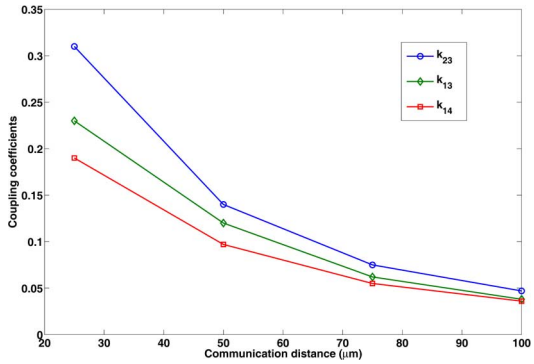


Fig. 4. Coupling coefficients with respect to different communication distances.

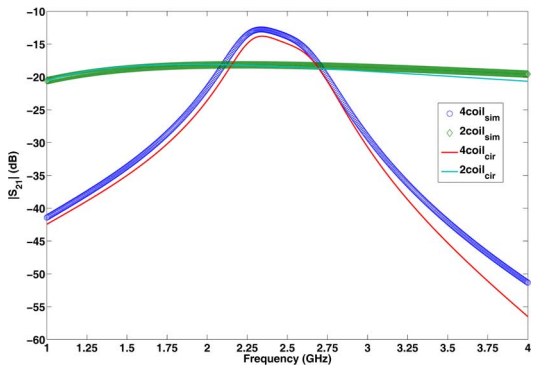


Fig. 5. $||S21||$ of the four-coil and two-coil systems obtained from HFSS simulation and equivalent circuit model.

TABLE I
GEOMETRIC SPECIFICATIONS OF THE TESTING STRUCTURE

| | |
|---|---|
| Outer diameter (D) | 100 $\mu m$ |
| Number of turns in spiral (Ns) | 5 |
| Width of conductor cross-section (w) | $2\mu m$ |
| thickness of conductor cross-section (t) | $2\mu m$ |
| spacing between adjacent turns (s) | $1\mu m$ |
| distance between TX (RX) and drive (load) coils | $2\mu m$ |

structure for $d = 50$ $\mu$m. The curve for traditional inductive coupling scheme is also simulated for comparison. The inductive coupling structure consists of only the TX and RX coils, to which the source and load are connected directly. The resonant capacitors are also absent. In general, the two-coil inductive coupling has a flat transfer efficiency curve over frequency. In contrast, the efficiency of MRC 4-coil system is much higher in the neighborhood of resonant frequency, while much lower in regions far away from the resonant frequency. The maximum difference between the two curves is 5.4 dB, which means that the input power at the transmitter at that particular frequency can be reduced by maximally 70% for the same power strength at the receiver end by using the four-coil structure. The $|S_{21}|$ curves predicted by the equivalent circuit model in Fig. 3 with the extracted parameters are also shown in Fig. 5, and good agreement is obtained.

The advantage of the MRC technique in maintaining a relatively high energy transfer efficiency over a large distance is further demonstrated in Fig. 6, which shows how the peak transfer efficiency of the MRC and inductive coupling varies

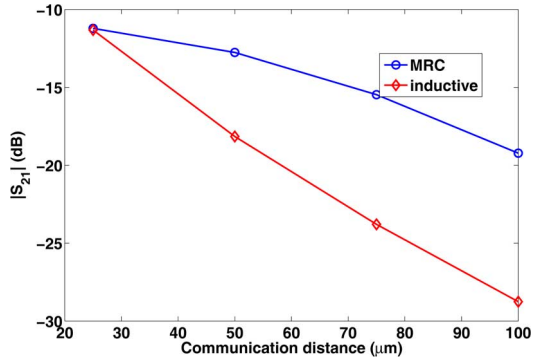


Fig. 6. Dependence of peak $||S21||$ of MRC and normal inductive systems on communication distance.

TABLE II
$-20$ dB BANDWIDTH OF INDUCTIVE COUPLING AND MRC FOR DIFFERENT DISTANCES

| Distance ($\mu m$) | inductive coupling | MRC |
|---|---|---|
| 25 | >5GHz | 1.2GHz |
| 50 | 3.9GHz | 700MHz |
| 75 | N/A | 400MHz |
| 100 | N/A | 150MHz |

with respect to the communication distance. The inductive coupling efficiency relies mainly on the magnetic coupling coefficient $k_{23}$, and drops rapidly as the coupling strength reduces $1/d^3$ along with the distance. When transmitting signal across multiple substrates in inter-chip communication, large size inductors (or a number of small-sized inductor arrays) are often required to generate sufficient power level at the receiver side. Meanwhile, the thickness of semiconductor substrates is required to be polished, in some cases down to 10 $\mu$m, so as to reduce the total communication distance and the eddy current effect. In the MRC transfer, however, the reduction in coupling coefficient can be compensated by the high $Q$ factors of the TX and RX coils [2], [7], [8]. Therefore, the restriction in distance and substrate thickness can be largely alleviated by a higher transfer efficiency.

Frequency bandwidth is another important factor in on-chip communication. In general, the MRC technique has a narrower bandwidth than that of inductive coupling for the same configurations, due to the requirement of a high $Q$ factor that is anti-proportional to the bandwidth of a resonant system. This suggests that the MRC technique will be more suitable for the scenarios where bandwidth is not a major concern. The absolute bandwidths of MRC and inductive coupling measured at $-20$ dB (representing 10 mW power received for 1 W transmitted power) are shown in Table II. It should be noted that, by allowing a tradeoff between $Q$ factor (power transfer efficiency) and bandwidth, the MRC technique actually provides more design flexibility than pure inductive coupling schemes. The efficiency of inductive coupling is mainly a function of the coupling coefficient as the $Q$ factors of coils are limited by the source and load resistances. The enhancement of coupling coefficient requires increasing the coil size and/or reducing the communication distance, which may be difficult in some circumstances. The $Q$ factor of coils in MRC, on the other hand, can be adjusted more conveniently through modifying the coil

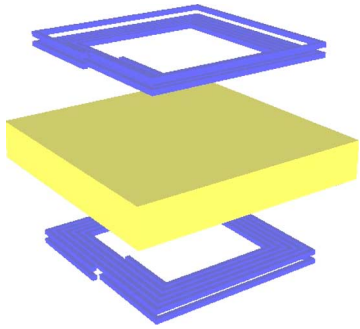

Fig. 7. Simulation model in Magwel.

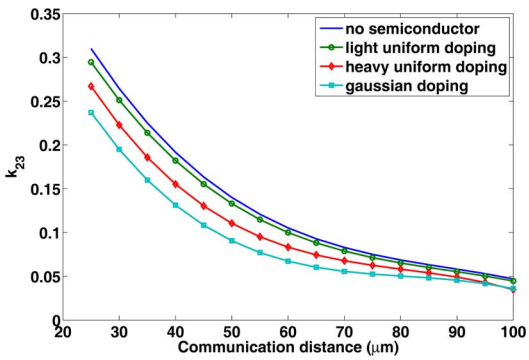


Fig. 8. $k_{23}$ vs. communication distance for different doping profiles.

layout, to achieve higher values for better power efficiency or lower values for bandwidth considerations.

## IV. EM-TCAD Simulation With Semiconductor Substrate

In this section, the impact of semiconducting substrate on the magnetic coupling is analyzed by the Magwel EM-TCAD simulator. The loss caused by the induced eddy current in semiconductor is quantified by a reduction of the coupling coefficient, which in turn decreases the transfer efficiency. We in this paper focus on the effect of different doping profiles of the semiconductor, which largely affects the substrate conductivity but is difficult to be accounted in conventional EM solvers. The simulation structure is depicted in Fig. 7. The two coils are of the same specifications as in Table I. A p-type silicon substrate of 20 $\mu$m thickness is inserted between the coils. The coupling coefficient (essentially $k_{23}$) is measured as indicated before for three different doping profiles: 1) uniform light doping (dopant concentration $N_p = 10^{15}$ cm$^{-1}$, 2) uniform heavy doping of $N_p = 10^{18}$ cm$^{-1}$ and 3) gaussian doping (where $N_p$ varies in the vertical direction according to the gaussian distribution).

The measured $k_{23}$ vs. distance curves are shown in Fig. 8. The curve without semiconductor is also shown for reference. It is seen that the presence of semiconductor substrate reduces the coupling coefficient due to the induced eddy currents. For lightly doped substrate, of which the conductivity is low, the coupling coefficient is affected only slightly. When high substrate conductivity results from the heavy doping, the coupling coefficient experiences a significant reduction due to the large eddy current. The deviation between the curves for uniform doping and gaussian doping highlights the necessity of using the EM-TCAD solver, since such difference cannot be captured in conventional EM simulator using the equivalent conductivity model for semiconductors.

## V. Conclusion

This paper investigates the feasibility of using a new wireless energy transfer technique, the MRC technique, to enhance the performance of traditional inductive coupling for inter-chip communication in 3D ICs. Numerical EM simulation and equivalent circuit analysis are conducted to demonstrate the advantages of MRC in terms of transfer efficiency. The reduction of magnetic coupling resulting from semiconductor substrates, which is unique for the studied application, is properly captured by the new EM-TCAD simulator. It has been shown that the MRC technique can be a promising substitute for inductive coupling and it is necessary to use advanced coupled simulation tools to take into account the field-carrier interplay. Future research directions include remedies to increase the bandwidth and optimized design for on-chip MRC system.

## Acknowledgment

This work was supported in part by The Hong Kong Polytechnic University under Grant G-U892.

## References

[1] A. Kurs, A. Karalis, R. Moffatt, J. D. Joannopoulos, P. Fisher, and M. Soljacic, "Wireless power transfer via strongly coupled magnetic resonances," *Science*, vol. 317, pp. 83–86, July 2007.

[2] B. L. Cannon, J. F. Hoburg, D. D. Stancil, and S. C. Goldstein, "Magnetic resonant coupling as a potential means for wireless power transfer to multiple small receivers," *IEEE Trans. Power Electron.*, vol. 24, no. 7, pp. 1819–1825, Jul. 2009.

[3] A. Kumar, S. Mirabbasi, and M. Chiao, "Resonance-based wireless power delivery for implantable devices," in *Proc. IEEE Biomedical Circuits and Systems Conf.*, Nov. 2009, pp. 25–28.

[4] N. Miura, D. Mizoguchi, M. Inoue, T. Sakurai, and T. Kuroda, "A 195-gb/s 1.2-W inductive inter-chip wireless superconnect with transmit power control scheme for 3-D-stacked system in a package," *IEEE J. Solid-State Circuits*, vol. 41, no. 1, pp. 23–34, Jan. 2006.

[5] A. Karalis, J. D. Joannopoulos, and M. Soljacic, "Efficient wireless non-radiative mid-range energy transfer," *Ann. Phys.*, vol. 323, no. 1, pp. 34–48, Jan. 2008.

[6] S. S. Mohan, M. Hershenson, S. P. Boyd, and T. H. Lee, "Simple accurate expressions for planar spiral inductances," *IEEE J. Solid-State Circuits*, vol. 34, no. 10, pp. 1419–1424, Oct. 1999.

[7] A. K. RamRakhyani, S. Mirabbasi, and M. Chiao, "Design and optimization of resonance-based efficient wireless power delivery systems for biomedical implants," *IEEE Trans. Biomed. Circuits Syst.*, vol. 5, no. 1, pp. 48–63, Feb. 2011.

[8] A. P. Sample, D. A. Meyer, and J. R. Smith, "Analysis, experimental results, and range adaptation of magnetically coupled resonators for wireless power transfer," *IEEE Trans. Ind. Electron.*, vol. 58, no. 2, pp. 544–554, Feb. 2011.

[9] Magwel, [Online]. Available: [Online]. Available: http://www.magwel.com